# ChemComm

## Accepted Manuscript

This article can be cited before page numbers have been issued, to do this please use: J. Quílez-Bermejo, E. Morallon and D. Cazorla-Amorós, *Chem. Commun.*, 2018, DOI: 10.1039/C8CC02105H.


This is an Accepted Manuscript, which has been through the Royal Society of Chemistry peer review process and has been accepted for publication.

Accepted Manuscripts are published online shortly after acceptance, before technical editing, formatting and proof reading. Using this free service, authors can make their results available to the community, in citable form, before we publish the edited article. We will replace this Accepted Manuscript with the edited and formatted Advance Article as soon as it is available.

You can find more information about Accepted Manuscripts in the author guidelines.

Please note that technical editing may introduce minor changes to the text and/or graphics, which may alter content. The journal's standard Terms & Conditions and the ethical guidelines, outlined in our author and reviewer resource centre, still apply. In no event shall the Royal Society of Chemistry be held responsible for any errors or omissions in this Accepted Manuscript or any consequences arising from the use of any information it contains.

ROYAL SOCIETY OF CHEMISTRY

rsc.li/chemcomm

View Article Online
DOI: 10.1039/C8CC02105H

Journal Name

COMMUNICATION

# Oxygen-reduction catalysis of N-doped carbons prepared by heat treatment of polyaniline at over 1100 ºC.

Received 00th January 20xx,
Accepted 00th January 20xx

DOI: 10.1039/x0xx00000x

www.rsc.org/

Javier Quílez-Bermejo,[a] Emilia Morallón [b] and Diego Cazorla-Amorós [*a]

**Advanced catalysts for oxygen reduction reaction based on N-doped carbon materials have been designed by pyrolysis of polyaniline at temperatures above 1100ºC. The detailed characterization and computational calculations suggest that the conversion from pyridine to quaternary N in edge position at high temperatures is the responsible for the outstanding activity.**

Hydrogen fuel cells (FCs) and direct methanol FCs arise as a substitute for current internal combustion engines due to their high energy efficiency and the lack of pollutant emissions compared to traditional car engines[1]. One important issue that makes difficult its implementation is the use of platinum (Pt) as electrocatalyst in both the hydrogen (or methanol) oxidation and oxygen reduction reactions (ORR). The high cost and low abundance of this metal[2], which corresponds to one-third of the fuel cell total cost, makes necessary either to decrease the amount of Pt in the catalyst or to substitute it by another active catalyst. In addition, most of the Pt (almost 90% of total Pt in the FCs[3]) is used in the cathode due to the low rate of the ORR. Finally, deactivation due to metal nanoparticle agglomeration and poisoning by traces of carbon monoxide (present in hydrogen) or methanol, causes the decrease of the catalytic activity with life-time[2,4]. In this sense, recent research focuses on the development of new cathode catalysts which can make a substantial advantage towards fuel cells expansion[5]. Thus, new materials that can produce similar catalytic activity as Pt towards ORR have been developed[6–12].

N-doped carbon materials are one of the candidates to replace Pt in fuel cells[5]. As they do not contain metals, a dramatic reduction of the catalyst cost may result. In some cases, the Pt activity has almost been reached, but these materials are based on expensive chemical reagents, like graphene, and complex and expensive synthetic methods which increases the final catalyst cost[8,12]. Although the effect of the N on the carbon materials has been studied extensively, there is still a strong debate about the nature of N functionalities which generates an improvement in the catalytic activity towards ORR[13].

Polyaniline (PANI) has been employed as a precursor of carbon materials for its use as support of metal nanoparticles[9–11] because of its high amount of N functional groups and its interesting properties[14]. N-doped carbon materials derived from PANI have also been studied as metal-free catalysts[15–20]. However, their catalytic activity towards ORR is too low to be applied in a commercial fuel cell. All these works have synthesized carbon materials through the pyrolysis of PANI at temperatures lower than 1000ºC in inert atmosphere. Some exceptions can be found in the literature where the temperature used is higher than 1000ºC[21,22]. However, the use of templates modifies the structural order and the properties of the carbon materials, which may introduce differences in the effect of the heat treatment. Moreover, in these works, the presence of metal traces (Fe[21] and Mn[22]) cannot be discarded from the preparation method used.

[a] Departamento de Química Inorgánica and Instituto de Materiales, Universidad de Alicante
[b] Departamento de Química Física and Instituto de Materiales, Universidad de Alicante

† Electronic Supplementary Information (ESI) available. See
DOI: 10.1039/x0xx00000x

View Article Online
DOI: 10.1039/C8CC02105H




The present work studies the effect of heat treatment temperature on the catalytic activity. The key experimental parameter is the carbonization temperature and the use of metal-free PANI as N-doped carbon precursor. When the carbonization temperature is 1100 or 1200°C, the PANI-derived carbon materials show excellent catalytic properties towards ORR in alkaline conditions and very good stability with resistance to methanol poisoning. This makes these catalysts suitable for utilization in fuel cells that work at low temperature and in alkaline conditions (hydrogen, methanol, ethanol, etc.). This route is a facile, high yield and low-cost synthesis method of N-doped carbon materials from PANI which reach an ORR activity in alkaline electrolyte similar to commercial Pt.

PANI was synthesized by chemical polymerization (more details in Supporting Information –SI-) and heat treated in a tubular furnace at temperatures between 600 and 1200°C in a $N_2$ atmosphere. The final carbon material is named as PANI_X, being X the carbonization temperature used during the heat treatment. The yield is included in Table S1.

The $H_2O_2$ selectivity and ORR activity in 0.1 M KOH solution of the obtained carbon materials and a 20 wt % Pt/C reference catalyst are shown in Fig. 1A and Fig. 1B, respectively. The sample treated at low temperature (600°C) shows a poor activity and selectivity in ORR, which is very far from the commercial Pt catalyst. The $H_2O_2$ yield is higher than 90%, what makes impossible its use as electrocatalyst in ORR; however, it could be useful in $H_2O_2$ formation reaction[23]. At intermediate temperatures (800-900°C), the materials start to acquire better ORR activities. Despite their better catalytic activity towards ORR, these samples are still not adequate compared to the commercial catalyst. In these cases, a decrease in $H_2O_2$ yield, with values around 70-80%, is observed. At higher temperatures (≥1000°C) a remarkable improvement in ORR activity happens, and at T ≥ 1100°C, materials with excellent ORR activities are obtained, which are close to 20% Pt/Vulcan. On the other hand, the $H_2O_2$ yield of the PANI-derived carbon materials obtained at high temperature is very low in the useful potential range of the FCs (0.6 – 1.0 V) which prevents the formation of harmful by-products during the operation of fuel cells. Similar results are obtained when using argon atmosphere (Fig. S1). RDE experiments using graphite as a counter electrode (Fig. S2) are similar to those with RRDE.

Another major problem of the Pt based catalysts is the stability performance and the carbon monoxide and methanol poisoning. Methanol poisoning study was done because it is the easiest way to evaluate carbon monoxide poisoning (present in traces in hydrogen gas)[24]. The stability of PANI_1100 was evaluated under potentiostatic conditions (Fig. S3). The results are promising since the 20% Pt/Vulcan sample reaches 87% of its initial activity after 2 hours of reaction,

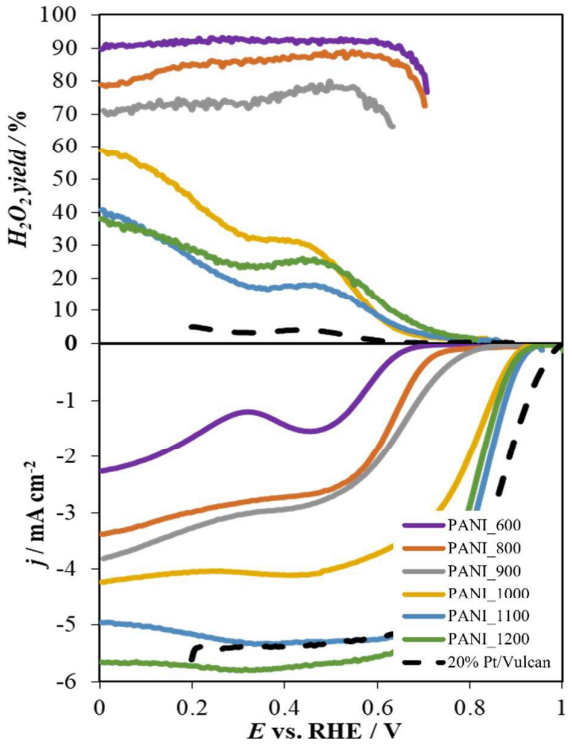


whereas PANI_1100 material has 95% of its initial activity after this reaction time. The methanol poisoning test was done by adding methanol to the electrolyte after 2 hours reaction (see the arrow in Fig. S3). Even after adding methanol, PANI_1100 activity is almost 90% of the initial value over 3 hours. However, the current of the 20wt% Pt/Vulcan sample drops to zero immediately after addition of methanol. The experiment supports that PANI-derived carbon materials are suitable in terms of stability and resistance towards methanol and carbon monoxide. Moreover, it can be a good candidate to be used in direct methanol fuel cells because of its tolerance to methanol poisoning. A detailed characterization of the materials was done to understand the reasons for their excellent catalytic activity towards ORR.

***Figure 1.*** *(a) $H_2O_2$ yield and (b) Linear sweep voltammetry curves for the prepared materials in $O_2$-saturated 0.1 M KOH at 5mV·s$^{-1}$ and 1600rpm.*

Fig. S4 shows the thermogravimetric analysis of PANI_1100 in air atmosphere. The material is completely burnt-off, showing its high purity and the lack of inorganic residues. The morphology and porosity of PANI-derived carbon materials were characterized by TEM and $N_2$ adsorption isotherms, respectively. TEM images (Fig. S5 and S6) show that the increase in heat treatment temperature does not produce a relevant increase in long-range structural order, but sheet-like structures are observed. Fig S7 shows that the there is a good development of porosity with heat treatment temperature. An explanation about these results are included in the SI. The surface area data show that it reaches the highest values for

View Article Online
DOI: 10.1039/C8CC02105H




heat treatment temperatures above 1000ºC. Thus, the increase in surface area is beneficial for increasing the catalytic activity[13]. However, since there is an additional improvement in catalytic activity when the heat treatment is done at 1100ºC or 1200ºC, the changes in structural order and chemical composition must play a relevant role in the catalytic activity.

Electrochemical impedance spectroscopy (Fig. S8) gives typical results for carbon-based materials. The size of the semicircle in the medium to high frequency range is related to the resistance of charge transfer through the grain-boundaries at the rough electrode-electrolyte interface[25,26] that allows dielectric polarization of the solution. In this sense, with increasing the heat treatment temperature, the diameter of the semicircle decreases what is indicative of the better electrical conductivity and charge propagation[27].

Raman spectra of all samples are presented in Fig. S9. The increase in temperature results in a narrowing of the D band and a displacement of G band towards higher wavelength reaching values closer to the D2 band. This band is associated to a lattice vibration analogous to that of the G band but involving graphene layers which are not directly sandwiched between two other graphene layers (i.e. 'boundary layer planes')[28–31]. Samples treated at 1100 and 1200 ºC have similar Raman spectra. This means that upon increasing the heat treatment temperature, the local structural order increases.

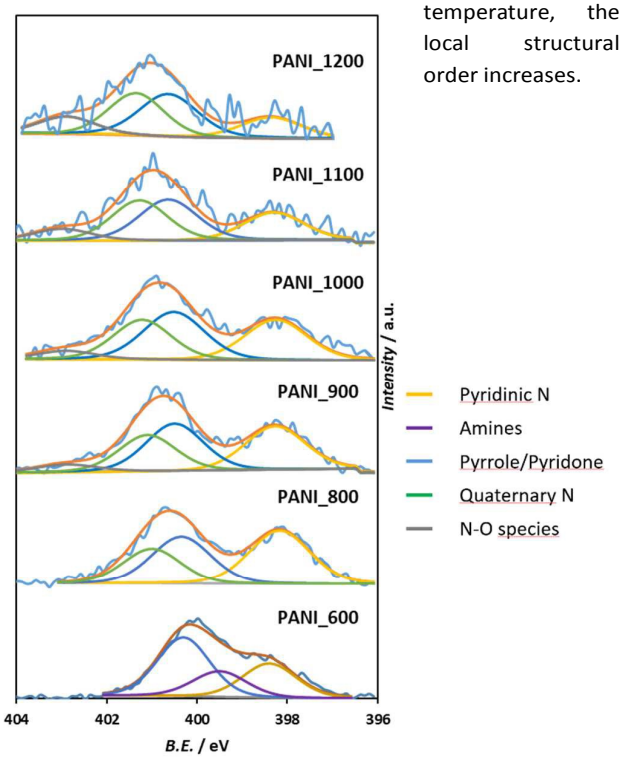


***Figure 2.*** *N1s spectra of all materials.*

However, in order to have a good ORR electrocatalytic activity in carbon materials, a good electrical conductivity, porosity and structural order are not enough to achieve excellent properties. For instance, pristine graphene does not present high activity towards ORR[8]. Thus, in addition to a good electron transfer from the cathode electrode, it is also necessary the presence of catalytically active sites, where the oxygen molecule is chemisorbed and reduced. In this sense, it is known that nitrogen (N) plays a fundamental role on ORR electroactivity[32] and that PANI-derived carbon materials contain a high amount of N-functionalities[14]. Thus, these functional groups can be the responsible for the creation of the catalytically active sites that produce the high activity observed for the materials treated at high temperature. Then, a detailed characterization of N species has been done. Fig. 2 shows N1s spectra of XPS for all materials prepared and Table S1 collects the quantification for each functionality detected. Low heat treatment temperatures produce pyridine, amines and pyrrole/pyridone species[33]. As temperature increases until 800-900ºC, a contribution of quaternary N appears and amines disappear due to its lower thermal stability[33]. Once a higher temperature (1000ºC) is reached, N-O species are observed and there is an important increase in quaternary N contribution while pyridine N species decrease and almost disappear in PANI_1200. Then, there is a conversion of pyridine to quaternary N due to condensation reactions that increase the size of the graphene layers[34].

From the $H_2O_2$ selectivity evolution (Fig. 1a), there is a change in $H_2O_2$ yield between samples treated at low-intermediate temperatures (i.e., 600-900ºC) and samples treated at high temperature (≥1000ºC). This suggests that the chemical nature of the species, which work as active sites towards ORR, changes with the increase in temperature during the treatment. The samples treated at high temperatures make the oxygen reduction via $4e^-$ (0% $H_2O_2$ yield) until ≃0,75V because of the presence of new active sites formed by high temperature treatment (these are named as species I). Below this potential, the $H_2O_2$ profile for this sample changes and the contribution of oxygen reduction via a $2e^-$ process increases. This suggests that less active species, which act as active sites in the samples treated at intermediate temperature (species II), that will also exist in high temperature samples, start to contribute to dioxygen reduction through the $2e^-$ mechanism producing an increase in $H_2O_2$ formation. Thus, there must exist a competition between the two actives sites for the $O_2$ reduction. In this sense, XPS analysis suggests that the modification of the nature of the active sites is due to the conversion of N pyridinic species to quaternary N and some small amount of oxidized N. Quaternary N species can activate the two contiguous carbon atoms that can constitute the

View Article Online
DOI: 10.1039/C8CC02105H




neighbour active sites that promote ORR through direct reduction to $H_2O$ (via $4e^-$)[20].

In order to gain a better understanding of the nature of these active sites, Fig. S10, S11, S12 and S13 show the model structure and the atom effective charge for the different possible functional groups that could work as active sites in the samples treated at high temperature. The arrows in these figures point out the two carbon atoms which can act as neighbour active sites, that are connected to a N atom and that could be responsible for the $4e^-$ $O_2$ reduction. In the case of N-O species (Fig. S10 and Fig. S11), the large negative charge in N-O functionality produces an important electron withdrawal in the carbon atoms, what may result in a strong chemisorption of $O_2$ and further carbon atom oxidation. This suggests that these groups do not work as efficient active sites for ORR. Moreover, if ORR could occur, it would be expected that in order to reduce the charge repulsion with the N-O species, the $O_2$ molecule would be preferentially chemisorbed on the positively charged carbon atom in a terminal configuration through one oxygen atom (Fig. S14), making the ORR on these groups preferentially via $2e^-$. A similar situation can be found in quaternary N species in armchair position (Fig. S12), where the asymmetric charge distribution for the neighbour C atoms and the high positive charge for one carbon atom, makes probable either the oxygen chemisorption and carbon oxidation or the $2e^-$ oxygen reduction route. However, in the case of quaternary N in zig-zag position (Fig: S13), the oxygen molecule could be bonded through the edges of the graphene plane, where the repulsion between $O_2$ and N atom will be reduced to the minimum and each oxygen atom would be adsorbed in a bridge configuration to the two positively charged (but weakly) carbon atoms (Fig. S15). This suggests that quaternary N in zig-zag position may produce the most active sites on carbon materials treated at high temperatures. Regarding quaternary N species, internal and edge functionalities should be differentiated. Whereas internal quaternary N species are considered as non active[32], edge-type quaternary N groups in zig-zag position have been proposed as active sites in the literature by computational modelling[32]. This means that the conversion at high temperatures (proposed in the literature[34]) from pyridinic N species to quaternary species at edge sites seems to be the responsible of the improvement in the catalytic activity towards ORR. It should be noted that pyridinic N does not seem to have a high activity towards ORR[32].

In summary, PANI heat treated at high temperatures in $N_2$ atmosphere produces excellent catalysts for ORR in alkaline electrolyte. The activity of the materials prepared at 1100°C is similar to that of 20wt% Pt/Vulcan and better than other N-doped carbon materials prepared by different methods or lower temperatures (see Table S2). The simple synthesis method makes these materials very promising for the future low-cost FCs commercialization. Moreover, we have proved that, the porosity, the electrical conductivity and structural order play a decisive role towards ORR. The pyridine functional group conversion to edge-type quaternary N species in zig-zag position during the heat treatment seems to be the responsible for the formation of the most active sites in PANI-derived carbon materials. The selection of the heat treatment temperature is crucial to achieve both an improved conductivity and the higher concentration of the most active, $4e^-$ catalytic active sites.

The authors thank MINECO of Spain and FEDER (CTQ2015-66080-R MINECO/FEDER).

## Conflicts of interest

There are no conflicts to declare

## Notes and references

1 B. C. Steele and A. Heinzel, *Nature*, 2001, **414**, 345–352.
2 I. E. L. Stephens, A. S. Bondarenko, U. Grønbjerg, J. Rossmeisl and I. Chorkendorff, *Energy Environ. Sci.*, 2012, **5**, 6744.
3 H. A. Gasteiger, J. E. Panels and S. G. Yan, *J. Power Sources*, 2004, **127**, 162–171.
4 N. Travitsky, L. Burstein, Y. Rosenberg and E. Peled, *J. Power Sources*, 2009, **194**, 161–167.
5 A. Morozan, B. Jousselme and S. Palacin, *Energy Environ. Sci.*, 2011, **4**, 1238.
6 J. Zhang, M. B. Vukmirovic, Y. Xu, M. Mavrikakis and R. R. Adzic, *Angew. Chemie - Int. Ed.*, 2005, **44**, 2132–2135.
7 F. Jaouen, E. Proietti, M. Lefèvre, R. Chenitz, J.-P. Dodelet, G. Wu, H. T. Chung, et. al., *Energy Environ. Sci.*, 2011, **4**, 114–130.
8 Z.-J. Lu, S.-J. Bao, Y.-T. Gou, C.-J. Cai, C.-C. Ji, M.-W. Xu, J. Song and R. Wang, *RSC Adv.*, 2013, **3**, 3990.
9 N. Gavrilov, I. A. Pašti, M. Mitrić, J. Travas-Sejdić, G. Ćirić-Marjanović and S. V. Mentus, *J. Power Sources*, 2012, **220**, 306–316.
10 H. W. Liang, W. Wei, Z. S. Wu, X. Feng and K. Müllen, J. Am. Chem. Soc., 2013, 135, 16002–16005.
11 G. Wu, K. L. More, C. M. Johnston and P. Zelenay, Science, 2011, 332, 443–447.
12 K. Gong, F. Du, Z. Xia, M. Durstock, K. Dai, Science, 2009, 323, 760-764.
13 K. H. Wu, D. W. Wang, D. S. Su and I. R. Gentle, ChemSusChem, 2015, 8, 2772–2788.
14 G. Ćirić-Marjanović, I. Pašti, N. Gavrilov, A. Janošević and S. Mentus, Chem. Pap., 2013, 67, 781–813.
15 R. Silva, D. Voiry, M. Chhowalla and T. Asefa, J. Am. Chem. Soc., 2013, 135, 7823–7826.
16 J. Zhang, Z. Zhao, Z. Xia and L. Dai, Nat. Nanotechnol., 2015, 10, 444–452.
17 F. Zhou, G. Wang, F. Huang, Y. Zhang and M. Pan, Electrochim. Acta, 2017, 257, 73–81.
18 A. Zhao, J. Masa, M. Muhler, W. Schuhmann and W. Xia, Electrochim. Acta, 2013, 98, 139–145.
19 L. Lai, J. R. Potts, D. Zhan, L. Wang, C. K. Poh, C. Tang, H. Gong, Z. Shen, J. Lin and R. S. Ruoff, Energy Environ. Sci., 2012, 5, 7936.
20 J. Quílez-Bermejo, C. González-Gaitán, E. Morallón and D. Cazorla-

View Article Online
DOI: 10.1039/C8CC02105H


Amorós, *Carbon*, 2017, **119**, 62–71.
21 K. Wan, Z.-P. Yu and Z.-X. Liang, *Catalysts*, 2015, **5**, 1034–1045.
22 W. Gao, D. Havas, S. Gupta, Q. Pan, N. He, H. Zhang, H.-L. Wang and G. Wu, *Carbon*, 2016, **102**, 346–356.
23 C. M. Sa and A. J. Bard, 2009, **81**, 8094–8100.
24 Q. Li, R. He, J. O. Jensen and N. J. Bjerrum, *Chem. Mater.*, 2003, **15**, 4896–4915.
25 D. Salinas-Torres, R. Ruiz-Rosas, M. J. Valero-Romero, J. Rodríguez-Mirasol, T. Cordero, E. Morallón and D. Cazorla-Amorós, *J. Power Sources*, 2016, **326**, 641–651.
26 P. Kurzweil, A. Hildebrand and M. Weiß, *ChemElectroChem*, 2015, **2**, 150–159.
27 R. Kötz and M. Carlen, *Electrochim. Acta*, 2000, **45**, 2483–2498.
28 S. Leyva-García, K. Nueangnoraj, D. Lozano-Castelló, H. Nishihara, T. Kyotani, E. Morallón and D. Cazorla-Amorós, *Carbon*, 2015, **89**, 63–73.
29 R. J. Bowling, R. T. Packard and R. L. McCreery, *J. Am. Chem. Soc.*, 1989, **111**, 1217–1223.
30 J. Schwan, S. Ulrich, V. Batori, H. Ehrhardt and S. R. P. Silva, *J. Appl. Phys.*, 1996, **80**, 440–447.
31 A. Sadezky, H. Muckenhuber, H. Grothe, R. Niessner and U. Pöschl, *Carbon*, 2005, **43**, 1731–1742.
32 T. Ikeda, M. Boero, S. F. Huang, K. Terakura, M. Oshima and J. Ozaki, *J. Phys. Chem. C*, 2008, **112**, 14706–14709.
33 S. Kuroki, Y. Hosaka and C. Yamauchi, *Carbon*, 2013, **55**, 160–167.
34 J. R. Pels, F. Kapteijn, J. A. Moulijn, Q. Zhu and K. M. Thomas, *Carbon*, 1995, **33**, 1641–1653.